

Optical parametric oscillator based on four-wave mixing in microstructure fiber

Jay E. Sharping, Marco Fiorentino, and Prem Kumar

Center for Photonic Communication and Computing, Northwestern University, 2145 Sheridan Road, Evanston, Illinois 60208-3118

Robert S. Windeler

OFS Laboratories, 700 Mountain Avenue, Murray Hill, New Jersey, 07974

Received April 22, 2002

We demonstrate, for the first time to our knowledge, optical parametric oscillation based on four-wave mixing in microstructure fiber. The measured wavelength-tunability range of the device (40 nm) and the threshold-pump peak power (34.4 W) are in good agreement with the theory of four-wave mixing in optical fibers. The ellipticity of the fiber's polarization modes allows the device to be implemented in a relatively simple Fabry-Perot configuration. Spectral peaks that are due to cascaded-mixing processes are easily observed in our setup, which may provide a way to extend the tunability range of existing high-power lasers. © 2002 Optical Society of America

OCIS codes: 060.2320, 060.4370, 190.4380, 190.4970.

Since the fabrication of "endlessly single-mode fiber"¹ there has been an ongoing search for applications that rely on the unique properties of these microstructure fibers (MFs). The demonstration of supercontinuum generation by Ranka *et al.*² has resulted in a flurry of research dedicated to understanding, in detail, the key mechanisms and design parameters that affect the propagation of light in MFs. Investigations into linear-optic effects such as dispersion,^{3,4} and birefringence⁵ and into nonlinear-optic effects⁶ such as Raman self-soliton generation,⁷ four-wave mixing,⁸ cross-phase-modulation induced switching,⁹ and third-harmonic generation¹⁰ have contributed to the rapid development of this field.

In this Letter we report what we believe to be the first demonstration of a MF-based optical parametric oscillator (MFOPO), in which the gain results from phase-matched four-wave mixing (FWM) in the MF. By pumping near the MF's zero-dispersion wavelength (λ_0) we obtain tunable radiation at wavelengths shorter than that of the pump. Cascaded FWM is also observed, wherein the oscillating signal, the pump, and the idler mix to create radiation at new wavelengths that are both longer and shorter than that of the pump. We evaluate the performance of the MFOPO in terms of its wavelength tunability and oscillation pump-power threshold. We also discuss how the polarization-mode behavior of the MF allows the system to oscillate in a relatively simple configuration. In addition, our experiment provides a detailed study of one of the nonlinear processes that occur below the supercontinuum threshold.

One promising aspect of this device is that it demonstrates the feasibility of building a tunable source where one may not already be available, especially in the blue-green region of the spectrum. Optical parametric oscillators (OPOs) based on $\chi^{(2)}$ nonlinearities are commonly used to build tunable sources, but generating radiation in the blue-green portion of the spectrum requires multiple nonlinear interactions (typically second-harmonic generation in conjunction with parametric downconversion).

Previously demonstrated fiber-based OPOs¹¹ required hundreds of meters of fiber and were restricted to operating at wavelengths near the λ_0 of conventional dispersion-shifted fibers (i.e., 1300–1600 nm). Much attention has been paid to the new flexibility available in MFs to tailor the waveguide component of the group-velocity dispersion⁴ (GVD), and MFs have been fabricated with values of λ_0 that ranged from 550 to 1550 nm.^{12,13} Using an appropriately tailored MF whose λ_0 is close to the wavelength of an existing high-power laser source, one can design a tunable MFOPO about that wavelength. The tunable range of the MFOPO depends on the slope of the GVD near λ_0 , so it is possible that by varying the GVD slope one could construct a more broadly tunable source.

FWM in MFs has already been demonstrated.¹⁰ For a given pump angular frequency ω_p and for the nonlinear refractive index of glass, $n_2 = 2.8 \times 10^{-20} \text{ m}^2/\text{W}$, the nonlinear coefficient $\gamma = n_2 \omega_p / A_{\text{eff}} c$ is enhanced by use of MFs, which have a very small effective mode area A_{eff} . Under the assumption of a strong pump, the phase-matching condition for FWM can be written as $\kappa = 2\gamma P_p - (2\pi c) D[(\omega_s - \omega_p)/\omega_p]^2 = 0$, where β_2 is the GVD coefficient and ω_s is the angular frequency of the signal. When a strong pump beam interacts with a weak signal beam under the phase-matching conditions, one observes amplification of the signal beam and generation of an idler beam of angular frequency, $\omega_i = 2\omega_p - \omega_s$. The primary factors that influence the FWM gain are γ , β_2 , the pump power, and the interaction length. In practice, the interaction length is the shortest of the fiber length, the loss length, and the walk-off length¹⁴; the fiber length is the operative length in our experiment. Near λ_0 , one can achieve a small but positive D , which, when coupled with a small amount of self-phase modulation on the pump, results in $\kappa \approx 0$. Use of this parametric gain mechanism in conjunction with efficient wavelength-selective feedback results in a tunable OPO.¹¹

The 2.1 m-long MF used in the experiments reported here was fabricated at OFS Laboratories.² It consists of an $\sim 2.1\text{-}\mu\text{m}$ -diameter silica core surrounded

by a hexagonal array of $\sim 1.4\text{-}\mu\text{m}$ -diameter air voids. We measured the attenuation coefficient, α , to be 0.02 m^{-1} (86 dB/km) by comparing the insertion losses for two different MF lengths. This fiber exhibits polarization-maintaining behavior owing to form birefringence⁵ as a result of a slight ellipticity of the core. We measured the fiber's λ_0 (Fig. 1, inset), and it turned out to be slightly different for the two polarization modes of this fiber.¹⁵

The birefringence behavior of a MF is made complicated by the presence of structural defects such as slight twists in the microstructure. It is highly likely that the polarization eigenmodes are elliptically rather than linearly polarized and that their ellipticity may also depend on wavelength, a phenomenon known as second-order polarization-mode dispersion in the context of telecommunication fibers. One can easily verify the presence of elliptical eigenmodes and second-order polarization-mode dispersion by observing changes in the polarization state after a single pass through the MF as the input polarization state and the wavelength are varied. Typically, injection of linearly polarized light into our MF results in a maximum of $\sim 86\%$ of the power in the fiber being coupled into the desired eigenmode, with the remaining 14% leaking into the other eigenmode. The fraction of light coupled into the desired mode does not vary as the fiber loops are moved, because of the polarization-maintaining ability of the MF. One verifies the presence of second-order polarization-mode dispersion by changing the wavelength of the input light and observing that the direction of input polarization must also be slightly adjusted to return to the optimum setting.

The MFOPO setup is shown schematically in Fig. 1. The pump, which is derived from a Ti:sapphire laser (Coherent, Inc., Model Mira 900), consists of a 75-MHz train of approximately Gaussian-shaped pulses with a temporal width of 630 ± 10 fs FWHM and a spectral width of 1.9 ± 0.1 nm, giving a time-bandwidth product of 0.64 ± 0.03 . The wavelength of the pump is widely tunable from $\sim 0.7\text{ }\mu\text{m}$ to $\sim 1\text{ }\mu\text{m}$. The MF is placed within a Fabry-Perot cavity that has a movable high reflector on one end and a diffraction grating in the Littrow configuration on the other. The use of 2.1 m of MF results in a MFOPO cavity whose longitudinal mode spacing is exactly half that of the pump source. Thus the system operates as a synchronously pumped harmonically mode-locked oscillator with output at the same 75-MHz repetition rate as that of the pump laser. Use of a polarization beam splitter (PBS) allows us to conveniently inject a strong pump beam, while the signal beam oscillates between the high reflector and the diffraction grating (see Fig. 1). A zero-order half-wave plate ($\lambda/2$) is used in the cavity to vary the polarization of the input pump beam with respect to the polarization-mode axes of the MF. A quarter-wave plate ($\lambda/4$) is placed between the polarization beam splitter and the diffraction grating to provide for a variable output coupling.

Figure 2 shows the power recorded at the signal output port (see Fig. 1) versus the pump power coupled into the MF. The oscillation threshold behavior is clearly seen when the pump's peak power exceeds

34.4 W (1.67-mW average power). The inset in Fig. 2 shows a typical optical spectrum measured at the cavity-monitor port for a pump wavelength of 751.8 nm. We can observe peaks that are due to the residual pump, to the oscillating signal (with the cavity length tuned for oscillation at 765.9 nm), and to the generated idler at 737.9 nm. Cascaded FWM is also observed, which leads to the peaks at 725 and 780 nm. The small dip in the center of the pump peak gives clear evidence of the self-phase modulation of the pump.

Figure 3 shows a composite of the output spectra recorded at the cavity-monitor port for various settings of the grating and the high reflector, revealing the tunability of the MFOPO. The peaks (lighter solid curves) to the right and the left of the pump peak at 751.8 nm represent different oscillating signal wavelengths. We can tune the signal output over a 40-nm range by simply rotating the diffraction grating and moving the end mirror to compensate for the GVD-induced cavity-length change. We also observe spontaneous parametric fluorescence, labeled PF in Fig. 3, in the wings of the central pump peak (darker solid curve), which we obtained by blocking the MFOPO cavity near the grating. Such parametric fluorescence in dispersion-shifted fiber was recently used to demonstrate an all-fiber photon-pair source for quantum communications.¹⁶

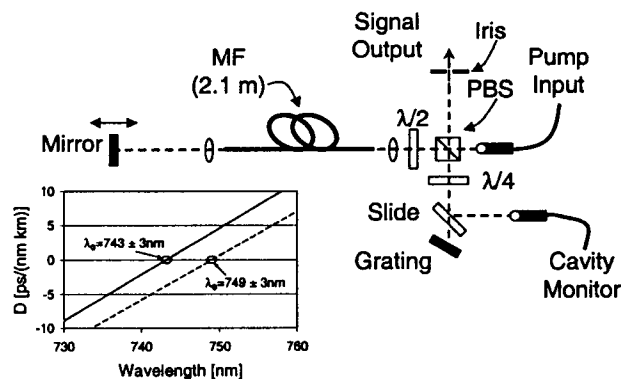


Fig. 1. Schematic of the MFOPO. Inset, measured wavelength dependence of GVD coefficient D in the vicinity of λ_0 for the two polarization modes of the MF.

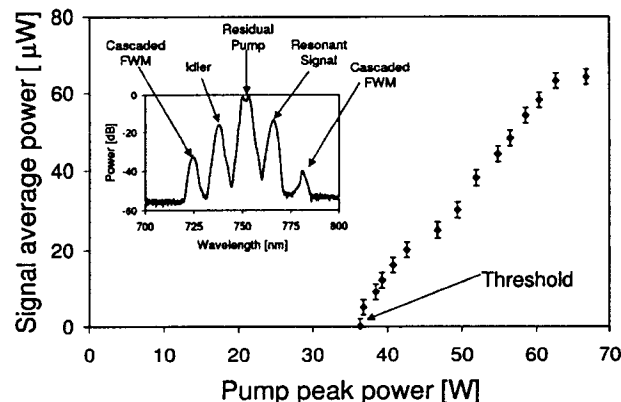


Fig. 2. Signal output average power versus pump peak power, showing the threshold behavior of the oscillator. Inset, typical intracavity spectrum.

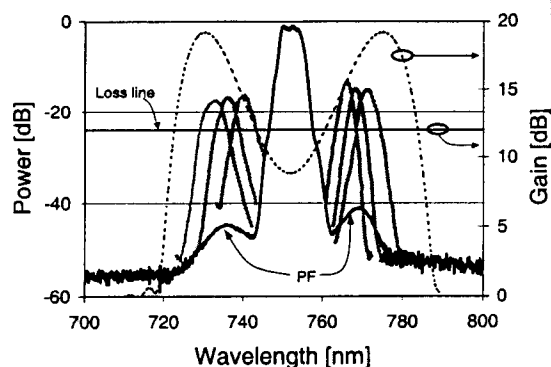


Fig. 3. Composite of the output spectra with oscillating signals at 733, 736, 740, 766, 768, and 772 nm (lighter solid curves). The darker solid curve shows the PF peaks with the MFOPO cavity blocked. Dashed curve, expected FWM small-signal gain spectrum.

The fact that there is sufficient mode overlap within the MF between the pump and the signal beams in the configuration of Fig. 1 is a consequence of the elliptical polarization-mode behavior of the MF. If one were to assume that the polarization eigenmodes of our MF were wavelength-independent linear-polarization states, it would be difficult to observe oscillation in the cavity configuration of Fig. 1, because the polarizations of the pump and signal would be orthogonal to each other. In principle, cross-polarization FWM is possible, but the nonlinear coefficient for such mixing is nine times smaller than that for copolarized FWM.¹⁴ In addition, there is a large group-velocity mismatch between the MF's polarization modes (1.7 ± 0.1 ps/m), which would further reduce the cross-polarized gain by shortening the effective interaction length. We experimentally verified that copolarized FWM is indeed the dominant gain mechanism by operating the MFOPO with an additional polarizer placed in the cavity near the high reflector.

For elliptical eigenmodes of the fiber, the orthogonal linear polarizations of the injected pump and the oscillating signal have copolarized projections onto the eigenmodes of the MF. The MFOPO oscillates when there is sufficient pump power to provide the needed FWM gain in a given eigenmode to offset the loss in the Fabry-Perot cavity. According to our measurements, we estimate the round-trip loss in the signal cavity to be 12 dB (round-trip transmissivity of 0.06 ± 0.01), wherein we have taken into account the round-trip MF transmissivity of 0.34 ± 0.05 (this includes round-trip coupling loss, Fresnel loss at each interface, and round-trip absorption loss in the fiber), the grating diffraction efficiency of 0.67 ± 0.02 , and the polarization-mode overlap of 0.29 ± 0.02 between the signal linear-polarization mode and the eigenmode of the MF.

The single-pass small-signal gain of the MFOPO was modeled by the technique described in Ref. 10. For a pump wavelength of 751.8 nm and a pump peak power equal to the threshold power of 34.4 W, the resultant gain is shown in Fig. 3 as a dashed curve. Other

parameters used in the model were $A_{\text{eff}} = 3.5 \mu\text{m}^2$ and $D = 1.8$ ps/(nm km). The peak calculated small-signal gain of 19 dB is reasonable when it is compared with the measured 12-dB round-trip loss value. Also, the wavelength regions wherein the small-signal gain exceeds the round-trip loss are in very good agreement with the spans over which the signal oscillation is observed (see Fig. 3).

In summary, we have demonstrated an OPO whose gain is produced in a microstructure fiber. We believe that similar devices that use MFs whose dispersion and modal properties are modified in novel ways would be useful for extending the tunability range of existing high-power laser sources.

This research was supported in part by the U.S. Army Research Office under a Multidisciplinary University Research Initiative grant (DAAD19-00-1-0177, DAAD19-00-1-0469). J. E. Sharping's e-mail address is j-sharping@northwestern.edu.

References

1. T. A. Birks, J. C. Knight, and P. St. J. Russell, *Opt. Lett.* **22**, 961 (1997).
2. J. K. Ranka, R. S. Windeler, and A. J. Stentz, *Opt. Lett.* **25**, 25 (2000).
3. M. J. Gander, R. McBride, J. D. C. Jones, D. Mogilevtsev, T. A. Birks, J. C. Knight, and P. St. J. Russell, *Electron. Lett.* **35**, 63 (1999).
4. A. Ferrando, E. Sylvestre, P. Andres, J. Miret, and M. V. Andres, *Opt. Express* **9**, 687 (2001), <http://www.opticsexpress.org>.
5. A. Ortigosa-Blanch, J. C. Knight, W. J. Wadsworth, J. Arriaga, B. J. Mangan, T. A. Birks, and P. St. J. Russell, *Opt. Lett.* **25**, 1325 (2000).
6. N. G. R. Broderick, T. M. Monro, P. J. Bennett, and D. J. Richardson, *Opt. Lett.* **24**, 1395 (1999).
7. X. Liu, C. Xu, W. H. Knox, J. K. Chandalia, B. J. Eggleton, S. G. Kosinski, and R. S. Windeler, *Opt. Lett.* **26**, 358 (2001).
8. J. E. Sharping, M. Fiorentino, A. Coker, P. Kumar, and R. S. Windeler, *Opt. Lett.* **26**, 1048 (2001).
9. J. E. Sharping, M. Fiorentino, P. Kumar, and R. S. Windeler, *IEEE Photon. Technol. Lett.* **14**, 77 (2002).
10. F. G. Omenetto, A. Taylor, M. D. Moores, J. Arriaga, J. C. Knight, W. J. Wadsworth, and P. St. J. Russell, *Opt. Lett.* **26**, 1158 (2001).
11. D. K. Serkland and P. Kumar, *Opt. Lett.* **24**, 92 (1999).
12. J. C. Knight, J. Arriaga, T. A. Birks, A. Ortigosa-Blanch, W. J. Wadsworth, and P. St. J. Russell, *IEEE Photon Technol. Lett.* **12**, 807 (2000).
13. K. P. Hansen, J. R. Jensen, C. Jacobsen, H. R. Simonsen, J. Broeng, P. M. W. Skovgaard, A. Petersson, and A. Bjarklev, in *Optical Fiber Communication Conference (OFC)*, Vol. 37 of OSA Trends in Optics and Photonics Series (Optical Society of America, Washington, D.C., 2002), paper FA9.
14. G. P. Agrawal, *Nonlinear Fiber Optics*, 2nd ed. (Academic, San Diego, Calif., 1995).
15. D. Ouzounov, D. Homoelle, W. Zipfel, W. W. Webb, A. L. Gaeta, J. A. West, J. C. Fajardo, and K. W. Koch, *Opt. Commun.* **192**, 219 (2001).
16. M. Fiorentino, P. Voss, J. E. Sharping, and P. Kumar, *IEEE Photon. Technol. Lett.* **14**, 983 (2002).